function of RUB/NEDD8 modification in both plant and animal systems.

In yeast, the most abundant Rub1p-modified protein is Cdc53p (*14*). Genetic evidence suggests that Rub1p modification regulates the activity of SCF^{Cdc4}, the E3 responsible for conjugation of UBQ to the CDK inhibitor Sic1p at the G_1-to-S phase transition. It is possible that RUB1 has a similar function in plant cells. For example, the *Arabidopsis* F-box protein TIR1 may be part of an SCF complex that is required for the degradation of negative regulators of auxin response. RUB1 may modify the activity of this SCF, perhaps in response to auxin (*23*). A homolog of *CDC53* exists in *Arabidopsis*, and it will be interesting to see if CDC53 is a target of RUB1 conjugation in plants.

REFERENCES AND NOTES

1. H. Klee and M. A. Estelle, *Annu. Rev. Plant Physiol. Plant Mol. Biol.* **42**, 1529 (1990).
2. M. L. Evans, in *Hormonal Regulation of Development II*, vol. 10 of *Encyclopedia of Plant Physiology*, T. K. Scott, Ed. (Springer-Verlag, Berlin, 1984), pp. 23–79.
3. L. Hobbie and M. A. Estelle, *Plant Cell Environ.* **17**, 525 (1994); C. Timpte, C. Lincoln, F. B. Pickett, J. Turner, M. Estelle, *Plant J.* **8**, 561 (1995).
4. A. Cernac, C. Lincoln, D. Lammer, M. Estelle, *Development* **124**, 1583 (1997).
5. M. Ruegger *et al.*, *Genes Dev.* **12**, 198 (1998).
6. H. M. O. Leyser *et al.*, *Nature* **364**, 161 (1993).
7. N. M. Chow, J. R. Korenberg, X. W. Chen, R. Neve, *J. Biol. Chem.* **271**, 11339 (1996); M. Shayeghi, C. L. Doe, M. Tavassoli, F. Z. Watts, *Nucleic Acids Res.* **25**, 1162 (1997).
8. A. L. Haas and T. J. Siepmann, *FASEB J.* **11**, 1257 (1997).
9. A. Ciechanover, S. Elias, H. Heller, A. J. Hershko, *J. Biol. Chem.* **257**, 2537 (1982).
10. M. Hochstrasser, *Annu. Rev. Genet.* **30**, 405 (1996).
11. E. Johnson, J. I. Schwienhors, R. J. Donmen, G. Blobel, *EMBO J.* **16**, 5509 (1997).
12. R. Mahajan, C. Delphin, T. Guan, L. Gerace, F. Melchior, *Cell* **88**, 197 (1997).
13. S. Muller, M. J. Matunis, A. Dejean, *EMBO J.* **17**, 61 (1998).
14. D. Lammer *et al.*, *Genes Dev.* **12**, 914 (1998); D. Liakopoulos, G. Doenges, K. Matuschewski, S. Jentsch, *EMBO J.* **17**, 2208 (1998).
15. J. Callis, T. Carpenter, C. Sun, R. D. Vierstra, *Genetics* **139**, 921 (1995); S. Tan and J. Callis, unpublished results.
16. C. Lister and C. Dean, *Plant J.* **4**, 745 (1993).
17. We diluted 20 ml of saturated culture of XL1-blue bearing His_6-tagged-AXR1 or ECR1 in 200 ml of LB medium containing ampicillin (75 μg/ml) and grew it at 30°C for 2 hours. Isopropyl β-D-thiogalactoside was added to a final concentration of 0.5 mM, and the mixture was incubated for 4 hours. Cells were harvested, resuspended in 8 ml of TBS-T [20 mM Tris-Cl (pH 7.4), 150 mM NaCl, and 0.5% Tween-20], and sonicated to lyse the cells. Supernatant was portioned into aliquots and kept at −80°C. *Brassica napus* and mouse cDNAs encoding RUB1 (GenBank HO7679) and NEDD8 (GenBank D10918) were modified for insertion into pGEX-2TK, using polymerase chain reaction. *Arabidopsis thaliana* expresses a protein identical to *B. napus* RUB1 (J. Callis, unpublished data). The GST-RUB1 and GST-NEDD8 were expressed as described above. After purification of these recombinant proteins with the GST system (Pharmacia), they were labeled with ^{32}P using cyclic AMP kinase (Promega), and the fusion was cleaved with thrombin. The thiolester reactions contained AXR1 and ECR1 extracts, 1 mM ATP, 0.1 mM DTT, 10 mM $MgCl_2$ and ~200 cps of labeled protein. This mixture was incubated for 30 min at 23°C, and half of the reaction was stopped for 15 min with 4% SDS/10% glycerol and the other half with SDS/glycerol and 100 mM DTT.
18. J. C. del Pozo and M. Estelle, data not shown.
19. Five-day-old *Arabidopsis* seedlings were ground in liquid N_2, and proteins were extracted with 5 v/w in TBS-T. Total protein was precipitated with 100% saturated $(NH_4)_2SO_4$, resuspended in 1/10 volume of TBS, and dialyzed against TBS for 24 hours. The final volume was adjusted to 5% glycerol and kept at −80°C. Thiolester reactions contained approximately 30 μg/μl of plant protein, 2 mM ATP, 0.2 mM DTT, 10 mM $MgCl_2$, and ~400 cps of labeled RUB1. The reaction was performed at room temperature for 45 min and stopped as described (*13*).
20. AXR1 antiserum was prepared from rabbits by Pocono Rabbit Farm (Canadensis, PA), using recombinant AXR1 protein in an SDS gel slice [S. E. Perky, K. W. Nichols, D. E. Fernandez, *Plant Cell* **8**, 1977 (1996)].
21. T. Kamitani, K. Kito, H. P. Nguyen, E. T. H. Yeh, *J. Biol. Chem.* **272**, 28557 (1997).
22. S. Handeli and H. Weintraub, *Cell* **71**, 599 (1992); S. Handeli, personal communication.
23. W. M. Gray and M. Estelle, *Curr. Opin. Biotechnol.*, in press.
24. Single-letter abbreviations for the amino acid residues are as follows: A, Ala; C, Cys; D, Asp; E, Glu; F, Phe; G, Gly; H, His; I, Ile; K, Lys; L, Leu; M, Met; N, Asn; P, Pro; Q, Gln; R, Arg; S, Ser; T, Thr; V, Val; W, Trp; and Y, Tyr.

25. We thank J. Turner (J.C.d.P., C.T., M.E.), B. McArdle, and J. Martin (S.T., J.C) for technical assistance. Supported by NSF grant 93-06759 (J.C.) and NIH grant GM43644 (M.E.). J.C.d.P. was supported by a long-term fellowship from the Spanish Government.

2 March 1998; accepted 12 May 1998

Close Contacts with the Endoplasmic Reticulum as Determinants of Mitochondrial Ca^{2+} Responses

Rosario Rizzuto,* Paolo Pinton, Walter Carrington, Frederic S. Fay,† Kevin E. Fogarty, Lawrence M. Lifshitz, Richard A. Tuft, Tullio Pozzan

The spatial relation between mitochondria and endoplasmic reticulum (ER) in living HeLa cells was analyzed at high resolution in three dimensions with two differently colored, specifically targeted green fluorescent proteins. Numerous close contacts were observed between these organelles, and mitochondria in situ formed a largely interconnected, dynamic network. A Ca^{2+}-sensitive photoprotein targeted to the outer face of the inner mitochondrial membrane showed that, upon opening of the inositol 1,4,5-triphosphate (IP_3)–gated channels of the ER, the mitochondrial surface was exposed to a higher concentration of Ca^{2+} than was the bulk cytosol. These results emphasize the importance of cell architecture and the distribution of organelles in regulation of Ca^{2+} signaling.

Upon physiological stimulation with IP_3-generating agonists, mitochondria undergo an increase in the concentration of Ca^{2+} in the matrix ($[Ca^{2+}]_m$) (*1*), well in the range of the Ca^{2+} sensitivity of the matrix dehydrogenases (*2*). This process, besides playing a direct role in the control of organelle function, may contribute to the modulation of the cytosolic Ca^{2+} concentration ($[Ca^{2+}]_c$), by buffering $[Ca^{2+}]_c$ (*3*) or influencing its spatiotemporal pattern (*4*). The accumulation of Ca^{2+} by mitochondria is rapid, despite the low affinity of their transport mechanisms (*5*). Because mitochondria might respond to microdomains of high $[Ca^{2+}]$ that were generated in their proximity by the opening of the IP_3-gated channels (*1*), we conducted high-resolution imaging of mitochondria and of their relation with the intracellular Ca^{2+} store (the ER). We directly monitored the $[Ca^{2+}]$ sensed by the mitochondrial Ca^{2+} uptake systems by using a targeted aequorin chimera.

The combined use of green fluorescent protein (GFP) chimeras with distinct spectral and targeting properties allows identification of two different subcellular structures in living cells (*6*). We expressed the S65T GFP mutant targeted to mitochondria [mtGFP(S65T)] (*6*) in HeLa cells (*7*) and used a high-speed imaging system that allows a three-dimensional (3D) fluorescence image of high resolution to be obtained from computationally deblurred optical sections (*8*). The 3D images, derived from image stacks taken at 30-s intervals with a 60× objective (pixel size 133 nm), revealed that mitochondria form a largely interconnected "tubular" network that undergoes

R. Rizzuto, P. Pinton, T. Pozzan, Department of Biomedical Sciences and the National Research Council Center for the Study of Biomembranes, University of Padova, Via Colombo 3, 35121 Padova, Italy.
W. Carrington, F. S. Fay, K. E. Fogarty, L. M. Lifshitz, R. A. Tuft, Biomedical Imaging Group, University of Massachusetts Medical Center, Worcester, MA 01605, USA.

*To whom correspondence should be addressed. E-mail: rizzuto@civ.bio.unipd.it
†Deceased.

continuous rearrangement (Fig. 1A). Within 1 min of observation, both growth and retraction, as well as fusion to other portions of the network, were frequently observed (see arrow), indicating a high structural plasticity. In agreement with previous observations (*9*), the "mitochondrial network" was even more obvious when a portion of a mtGFP(S65T)-transfected cell was analyzed at higher resolution (Fig. 1B). The visual appearance of a connected network and the luminal continuity were confirmed by the rapid recovery of fluorescence after photobleaching of mtGFP in a portion of the network (Fig. 1C). Finally, to simultaneously visualize the mitochondria and the ER, we cotransfected in HeLa cells a mitochondrially targeted blue mutant of GFP, mtGFP(Y66H, Y145F) (*6*), and a chimera of GFP(S65T) targeted to the ER [erGFP(S65T)] (*10*) (Fig. 1D). Domains of close apposition were evident in Fig. 1D and in similar images. From these data, the surface of the mitochondrial network in close apposition to the ER was estimated to be ~5 to 20% of total (*11*).

On the basis of the morphological data, we expected that the microdomains of high $[Ca^{2+}]$ generated by the opening of the IP_3-gated channels might be sensed by only a small portion of the mitochondrial surface. To verify this possibility, we constructed an aequorin chimera targeted to the mitochondrial intermembrane space (MIMS) (*12*). This chimera (designated mimsAEQ), when transiently expressed in HeLa cells, appeared properly sorted, as shown by the pattern of the immunocytochemical stain (*13*) (Fig. 2A) and by results of dual-labeling experiments with the mitochondrial marker cytochrome *c* oxidase (*14*). The MIMS location of aequorin was confirmed by the characteristics of agonist-dependent $[Ca^{2+}]$ changes (*15*). Indeed, the peak $[Ca^{2+}]$ increase elicited by histamine, an IP_3-generating agonist (Fig. 2B), was much smaller than that measured in the mitochondrial matrix with mtAEQ (Fig. 2C) and was unaffected by treatment with the uncoupler carbonylcyanide *p*-(trifluoromethoxy) phenylhydrazone (FCCP), which collapses the driving force for Ca^{2+} uptake in the matrix (*16*).

The histamine-dependent $[Ca^{2+}]_{mims}$ changes differed also from those of $[Ca^{2+}]_c$. In particular, the initial maximal $[Ca^{2+}]_{mims}$ increase, which is mostly contributed by the release of Ca^{2+} from intracellular stores, exceeded that of $[Ca^{2+}]_c$ (3.5 ± 0.2 compared with 2.5 ± 0.3 μM, $n = 10$), and then declined to similar concentrations (Fig. 2D). Because the outer mitochondrial membrane is freely permeable to ions, a possible explanation of this finding is that a small fraction of the photoprotein is transiently exposed to a local domain of saturating $[Ca^{2+}]$ and is completely discharged. Thus, although the increase in $[Ca^{2+}]$ in most of the MIMS is in fact similar to that of the cytosol, the maximal light emission of this aequorin fraction contributes to the total luminescence signal; hence, the calibrated $[Ca^{2+}]_{mims}$ increase appears to be larger than that of $[Ca^{2+}]_c$. If this were the case, then, because of the irreversible photoprotein consumption in these domains, the difference in the apparent $[Ca^{2+}]$ of the two compartments would decrease during a subsequent agonist stimulation applied shortly after the first. Indeed, when the cells were exposed to another IP_3-generating agonist, adenosine triphosphate (ATP), after the stimulation with histamine, the difference in the peak $[Ca^{2+}]$ increase of the cytoplasm and of the MIMS was nearly abolished (*17*). The discrepancy between the increases in $[Ca^{2+}]_{mims}$ and $[Ca^{2+}]_c$ (Fig. 2D) is not a calibration artifact due either to an intrinsic difference in the Ca^{2+} affinity of the two chimeras or to local pH or pMg gradients. Indeed, using a membrane-bound cytosolic probe (mGluR1/AEQ) (*18*), we observed, in digitonin-permeabilized cells, that release of Ca^{2+} from the ER induced by the administration of IP_3 caused a greater increase in $[Ca^{2+}]$ in the MIMS than in the bulk cytosol, whereas perfusion of a buffered Ca^{2+} solution increased the $[Ca^{2+}]$ of the two compartments to the same extent (Fig. 2E).

At contacts between the ER and mitochondria, microdomains of high $[Ca^{2+}]$ may be generated upon opening of the IP_3-gated channels. These microdomains could allow

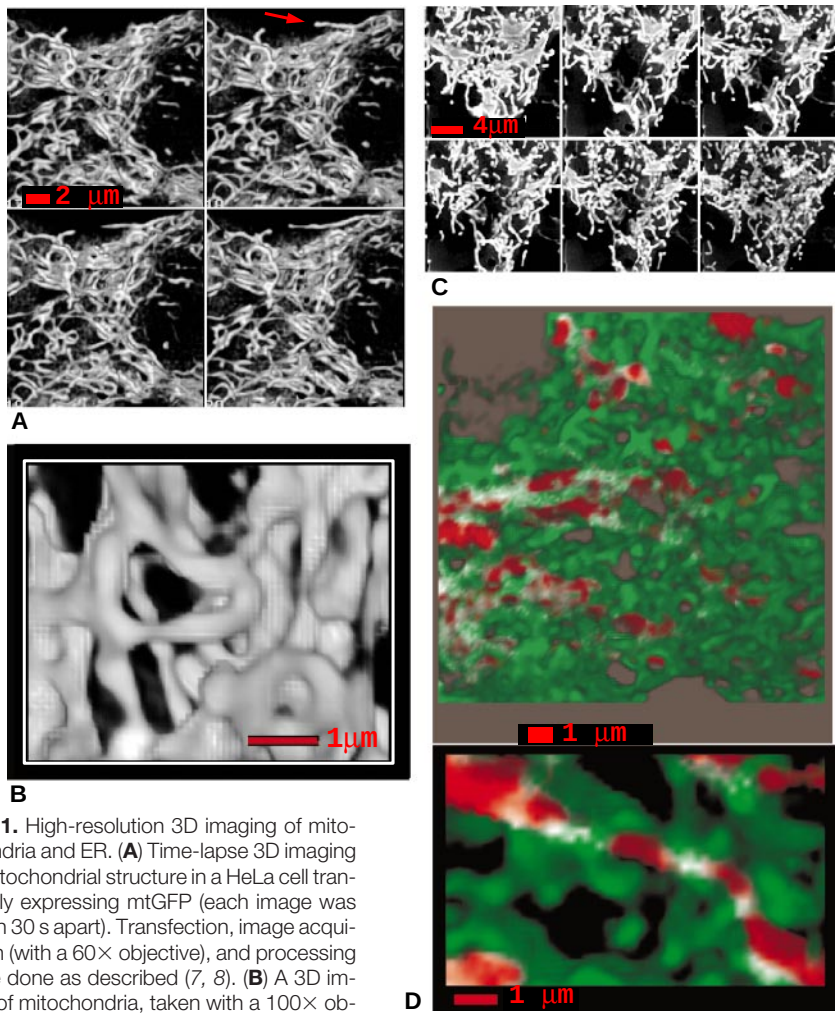

Fig. 1. High-resolution 3D imaging of mitochondria and ER. (**A**) Time-lapse 3D imaging of mitochondrial structure in a HeLa cell transiently expressing mtGFP (each image was taken 30 s apart). Transfection, image acquisition (with a 60× objective), and processing were done as described (*7, 8*). (**B**) A 3D image of mitochondria, taken with a 100× objective; all other experimental conditions as in (A). (**C**) Recovery of mtGFP fluorescence after photobleaching; experimental conditions as in (A). The first and second image were taken immediately before and after photobleaching mtGFP fluorescence in a small area within the cell. The following three images were taken at 2-min intervals after and the final image 30 min after the photobleaching. (**D**) Combined 3D imaging of mitochondria and ER in a HeLa cell transiently expressing mtGFP(Y66H,Y145F) and erGFP(S65T). The two 3D images were processed as in (A) and superimposed. The mitochondrial and ER images are represented in red and green, respectively; the overlaps of the two images are white. On the bottom, a detail of the main image (80-nm pixel).

the rapid uptake of a large amount of Ca^{2+} by mitochondria. The rapid diffusion of Ca^{2+} within the mitochondrial network (as revealed by the discharge of a major portion of mitochondrial matrix aequorin, mtAEQ) could allow the rapid tuning of mitochondrial metabolism to cell needs. On the cytosolic side, diffusion of Ca^{2+} would dissipate the microdomains, thus extending the Ca^{2+} signal to the bulk cytosol (and eliciting the cell response). The lower $[Ca^{2+}]$ would limit further accumulation into mitochondria, avoiding organelle overload, Ca^{2+} cycling, and collapse of the proton gradient.

On the basis of this model, we would predict that if a second release of Ca^{2+} from the ER is induced after the first, then because of the depletion of active aequorin in the mitochondrial regions closer to the ER, the apparent $[Ca^{2+}]_m$ increase should be underestimated. However, if enough time elapses between two consecutive stimulations, unconsumed mtAEQ should diffuse intralumenally from other regions of the mitochondrial network, leading to a larger increase in light emission, and thus the calibrated $[Ca^{2+}]_m$ increase should recover its initial amplitude. We treated cytosolic aequorin (cytAEQ)– or mtAEQ-transfected cells with ATP first, and then 1.5 or 10 min later, with histamine (Fig. 3). In the former case, the histamine-dependent $[Ca^{2+}]_m$ increase was smaller than the increase caused by ATP and drastically less than that observed in cells in which the ATP stimulation was omitted (43 ± 3%). The amplitudes of the $[Ca^{2+}]_m$ increases did not correlate with those of $[Ca^{2+}]_c$ (for example, in the second stimulation with histamine, the $[Ca^{2+}]_c$ increases were larger than those caused by ATP), but rather suggested that, during stimulation with a first agonist, mtAEQ was preferentially consumed at the "hotspots." In fact, if the second histamine treatment was given after a 10-min delay, the increase in $[Ca^{2+}]_m$ was larger, approaching the values measured when histamine was applied as first stimulus (84 ± 8%).

The observation that mitochondria form in vivo a largely connected, continuous network has consequences for understanding physiological events, such as organelle biogenesis and mitochondrial energy conservation, and for clarifying pathophysiological events, such as the mechanisms that lead to defects in mtDNA. Close appositions between ER and mitochondria may represent the site where microdomains of high $[Ca^{2+}]$ are generated upon IP_3-mediated Ca^{2+} release. Indeed, there is a good agreement between the area of the apposition sites and the area in which the increase in $[Ca^{2+}]$ saturated the binding of Ca^{2+} to aequorin (*19*). The microheterogeneity of the Ca^{2+} signal, and the spatial relation between ER and mitochondria, may thus be determinants of mitochondrial Ca^{2+} uptake, which influences organelle function (*1*) and may modulate the cytosolic Ca^{2+} signal (*2*, *3*).

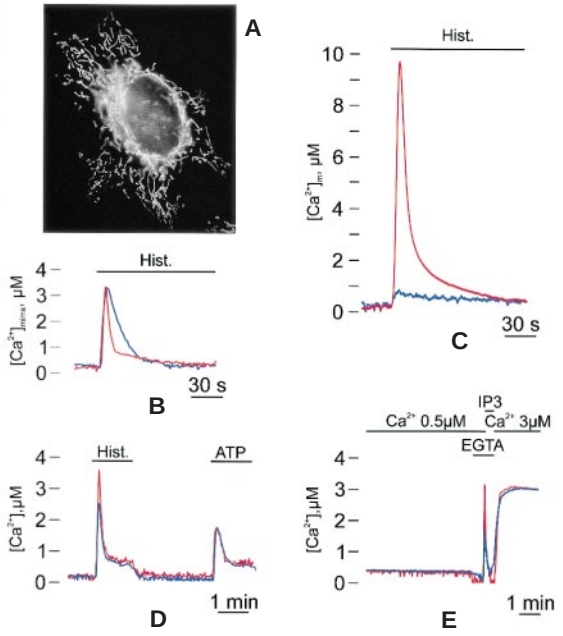

Fig. 2. An aequorin chimera targeted to the mitochondrial intermembrane space (mimsAEQ) reveals domains of high $[Ca^{2+}]$ upon IP_3-mediated Ca^{2+} release from the ER. (**A**) Immunolocalization of mimsAEQ in transiently transfected HeLa cells. The effect of mitochondrial uncoupling on the histamine-dependent increases in (**B**) $[Ca^{2+}]_{mims}$ and (**C**) $[Ca^{2+}]_m$. Both $[Ca^{2+}]_{mims}$ and $[Ca^{2+}]_m$ were monitored with mimsAEQ and mtAEQ, respectively. Red trace, control cells; blue trace, cells treated with 5 μM FCCP 1 min before addition of 100 μM histamine (Hist.). Traces [in (B) through (E), and in Fig. 3] are representative of at least five similar experiments. (**D**) Effect of repeated agonist stimulation on $[Ca^{2+}]_c$ and $[Ca^{2+}]_{mims}$. Transfected HeLa cells (red, mimsAEQ; blue, cAEQ) were treated with 100 μM histamine (Hist.) and 100 μM ATP. (**E**) IP_3-dependent $[Ca^{2+}]_{mims}$ and $[Ca^{2+}]_c$ changes in permeabilized cells. Transfected HeLa cells (red, mimsAEQ; blue, mGluR1/AEQ) were permeabilized with digitonin and perfused with IB, supplemented as specified (*15*). Where indicated (IP3), 5 μM IP_3 was added.

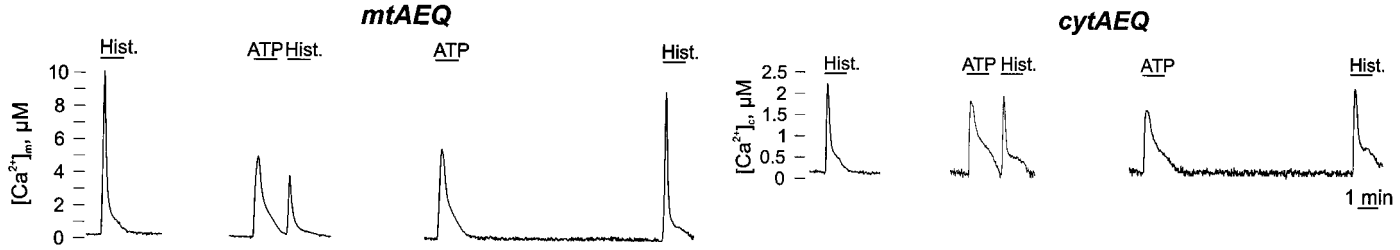

Fig. 3. Time-dependent recovery of mtAEQ luminescence during a second agonist stimulation. The value of $[Ca^{2+}]_m$ and, for comparison, the value of $[Ca^{2+}]_c$ were monitored in cells transfected with mtAEQ or cAEQ. All conditions as in Fig. 2. Where indicated, the cells were treated with 100 μM histamine (Hist.) or ATP.

REFERENCES AND NOTES

1. H. Miyata *et al*., *Am. J. Physiol.* **261**, H1123 (1991); R. Rizzuto *et al*., *Nature* **358**, 325 (1992); R. Rizzuto, M. Brini, M. Murgia, T. Pozzan, *Science* **262**, 744 (1993); A. M. Lawrie, R. Rizzuto, T. Pozzan, A. W. M. Simpson, *J. Biol. Chem.* **271**, 10753 (1996).
2. J. G. McCormack *et al*., *Physiol. Rev.* **70**, 391 (1990); R. G. Hansford, *J. Bioenerg. Biomembr.* **26**, 495 (1994); R. Rizzuto *et al*., *J. Cell Biol.* **126**, 1183 (1994); G. Hajnoczky *et al*., *Cell* **82**, 415 (1995); G. A. Rutter *et al*., *Proc. Natl. Acad. Sci. U.S.A.* **93**, 5489 (1996); L. D. Robb-Gaspers *et al*., unpublished data.
3. J. L. Werth and S. A. Thayer, *J. Neurosci.* **14**, 348 (1994); R. J. White and I. J. Reynolds, *ibid*., **15**, 1318 (1995); L. Kiedrowski and E. Costa, *Mol. Pharmacol.* **47**, 140 (1995); S. L. Budd and D. G. Nicholls, *J. Neurochem.* **66**, 403 (1996); J. Herrington *et al*., *Neuron* **16**, 219 (1996); R. M. Drummond and F. S. Fay, *Pfluegers Arch.* **431**, 473 (1996).
4. L. S. Jouaville *et al*., *Nature* **377**, 438 (1995).
5. E. Carafoli, *Annu. Rev. Biochem.* **56**, 395 (1987); T. Pozzan *et al*., *Physiol. Rev.* **74/3**, 595 (1994).
6. R. Heim and R. Y. Tsien, *Curr. Biol.* **6**, 178 (1996); R. Rizzuto *et al*., *ibid*., p. 183.
7. HeLa cells, grown in Dulbecco's modified Eagle's medium (DMEM), supplemented with 10% fetal calf serum (FCS), were seeded onto glass coverslips (diameter: 13 mm for aequorin measurements, 25 mm for GFP detection). Transfection with the appropriate plasmid was done as described [R. Rizzuto *et al*., *Methods Enzymol.* **260**, 417 (1995)].
8. The high-speed (30 ms/image) imaging system uses laser illumination and a low-noise frame transfer charge-coupled device camera (128 × 128 pixels,

540 frames/s, 70% quantum efficiency, six-electron readout noise). With a 20-ms exposure time and 10 ms to shift focus, 41 optical sections (*z* step-0.25 μm) of a mtGFP-transfected cell are obtained in ~1 s, a time scale in which mitochondrial motion is minimal. The wide-field images were deblurred and reconstructed in 3D as described [W. A. Carrington *et al*., *Science* **268**, 1483 (1995); R. Rizzuto, W. A. Carrington, R. A. Tuft, *Trends Cell Biol*., in press].
9. M. T. Davison and P. B. J. Garland, *J. Gen. Microbiol.* **98**, 147 (1977); L. E. Bakeeva *et al*., *Biochim. Biophys. Acta* **501**, 349 (1978); J. Bereiter-Hahn and M. Voth, *Microsc. Res. Tech.* **27(3)**, 198 (1994); C. L. Campbell *et al*., *Mol. Biol. Cell* **5**, 899 (1994); J. Nunnari *et al*., *ibid.* **8**, 1223 (1997).
10. The portion of the immunoglobulin heavy chain used for ER targeting (L-VDJ-CH1) was excised from erAEQ [M. Montero *et al*., *EMBO J.* **14**, 5467 (1995)] and cloned in the expression vector VR1012 in front of either GFPwt or GFP(S65T). The final constructs were designated erGFPwt or erGFP(S65T), respectively. The ER localization of both chimeras was confirmed by the colocalization with the ER marker calreticulin. Given the stronger fluorescence of erGFP(S65T), we used this construct for the experiment of Fig. 1. In double-labeling experiments with erGFP(S65T) and mtGFP(Y66H,Y145F), the sample was alternatively illuminated at each *z* section with ultraviolet and blue light, and the emitted light was filtered by a two-band filter. The two images were then independently collected and separately processed. Use of high-speed shutters kept the acquisition time of a 40-plane stack short (~2 s).
11. The ER and mitochondria images were separately thresholded over a range that eliminated background but preserved organellar structure. Subresolution functional overlap was determined from the percentage of mitochondria surface voxels that also contained ER; compensating for the limited resolution (which increases apparent overlap) increased the range of estimated overlap.
12. For constructing the mimsAEQ chimera, the Cla I–Eco RI fragment encoding hemagglutinin-1 (HA1)–tagged aequorin [M. Brini *et al*., *J. Biol. Chem.* **270**, 9896 (1995)] was inserted downstream of the internal Cla I site of the glycerol phosphate dehydrogenase (GPD) cDNA [L. J. Brown *et al*., *ibid.* **269**, 14363 (1994)]. The encoded polypeptide included amino acids 1 to 626 of GPD, the nine–amino acid HA1 tag [J. Field *et al*., *Mol. Cell. Biol.* **8**, 2159 (1988)], and aequorin. On the basis of the predicted structure of GPD [M. J. MacDonald and L. J. Brown, *Arch. Biochem. Biophys.* **326**, 79 (1996)], the aequorin moiety was expected to protrude into the mitochondrial intermembrane space and thus report the $[Ca^{2+}]$ changes occurring at the surface of the ion-impermeable inner mitochondrial membrane, which is where the low-affinity mitochondrial Ca^{2+} uniporter is located.
13. M. Brini *et al*., *J. Biol. Chem.* **270**, 9896 (1995); R. Rizzuto *et al*., *Methods Enzymol.* **260**, 417 (1995).
14. R. Rizzuto, P. Pinton, and T. Pozzan, data not shown.
15. After aequorin reconstitution, done as described (*12*), the cells were transferred to the luminometer chamber and perfused with modified Krebs-Ringer buffer (KRB): 125 mM NaCl, 5 mM KCl, 1 mM Na_3PO_4, 1 mM $MgSO_4$, 5.5 mM glucose, and 20 mM Hepes (pH 7.4, 37°C). All additions were then made to this buffer, as specified in the figure legends. In the experiment of Fig. 2E, we used an "intracellular" buffer (IB): 140 mM KCl, 10 mM NaCl, 1 mM K_3PO_4, 5.5 mM glucose, 2 mM $MgSO_4$, 1 mM ATP, 2 mM sodium succinate, and 20 mM Hepes (pH 7.05 at 37°C). As indicated in the figure, IB was supplemented with either 50 μM EGTA (free $[Ca^{2+}] < 10^{-8}$ M) (IB/EGTA) or an EGTA (2 mM)-buffered $[Ca^{2+}]$ of 0.5 μM (IB/0.5 μM Ca^{2+}) or 3 μM (IB/3 μM Ca^{2+}). Before the luminescence was recorded, transfected HeLa cells were permeabilized by a 1-min incubation with digitonin (added to IB/EGTA). The aequorin luminescence signal, collected by a low-noise photomultiplier, was converted off-line into $[Ca^{2+}]$ by an algorithm based on the Ca^{2+} affinity of aequorin at physiological conditions of pH, $[Mg^{2+}]$, ionic strength, and temperature (*12*).
16. In FCCP-treated cells, the return of $[Ca^{2+}]_{mims}$ to basal values, as well as that of $[Ca^{2+}]_c$ (*14*), was delayed.
17. In addition, no difference between the two compartments was observed when Ca^{2+} leaked out from the ER after inhibition of the ER Ca^{2+}–adenosine triphosphatase with 2,5-di(*tert*-butyl)-1,4-benzohydroquinone (tBuBHQ) [G. E. N. Kass *et al*., *J. Biol. Chem.* **264**, 15192 (1989)].
18. We generated mGluR1/AEQ by the fusion of aequorin to the COOH-terminus of a truncated metabotropic glutamate receptor (mGluR1). This chimeric aequorin, aimed at measuring $[Ca^{2+}]$ under the plasma membrane, was instead retained in the ER and the Golgi apparatus. mGluR1/AEQ is thus exposed to the $[Ca^{2+}]$ of the cytoplasm, while residing on the outer surface of internal membranes, and in fact reports the same $[Ca^{2+}]$ as cAEQ.
19. Comparison of the luminescence data of cAEQ and mimsAEQ allows a rough estimate of the domains at high $[Ca^{2+}]$ generated in the MIMS upon IP_3-dependent Ca^{2+} release from the ER. If the rate of discharge of cytAEQ closely matches that of the "bulk" MIMS, the difference between light emission of mimsAEQ and cAEQ (3 to 5%) can be attributed to the discharge of mimsAEQ in the domains at high $[Ca^{2+}]$. Assuming that the distribution of mimsAEQ was homogeneous and the $[Ca^{2+}]$ in these microdomains was high enough to cause complete discharge of all their aequorin content, the regions should correspond to ~3 to 5% of the MIMS.
20. We thank M. Murgia for constructing the erGFP(S65T) cDNA; R. Bisson, F. DiLisa, C. Montecucco, and G. Rutter for critically reading and discussing the manuscript; and J. Carmichael, G. Ronconi, and M. Santato for technical assistance. Supported by grants from Telethon (845, 850), from the Human Frontier Science Program, from the E. U. Biomed program (BMH4CT960181), from the Armenise Foundation (Harvard University), from the Italian University Ministry, and from the British Research Council to R.R. and T.P., by grants from NSF (DBI-9200027 and DBI-9724611) and NIH (HL14523 and RR09799) to W.C., F.S.F., K.E.F., L.M.L., and R.A.T.; and by a NATO Travel grant to R.R. and F.S.F. This report is dedicated to the memory of our dear friend and colleague Fredric S. Fay, whose enthusiasm and insights nurtured this collaboration, but who did not live to see its fruition.

6 February 1998; accepted 24 April 1998